Physical modeling of atmospheric boundary layer flows

Part IV: Modeling stably stratified boundary layer flows

Part V: Models of special boundary layer flows

Evgeni Fedorovich
School of Meteorology, University of Oklahoma, Norman, USA

Outline

- **Phenomenology of stably stratified boundary layer (SBL) flows**
- **Wind tunnel facilities to model atmospheric SBL**
- **Parameters to characterize turbulent SBL flows**
- **Results from a wind tunnel model of SBL**
  - Flow regime changes with increasing stability
  - Mean flow profiles and turbulence statistics in modeled SBLs
- **Wind tunnel modeling of flows inside/above plant canopies**
- **Wind tunnel modeling of urban boundary layer flows**
- **Concluding remarks**

Place of SBL in the diurnal cycle of atmospheric planetary boundary layer

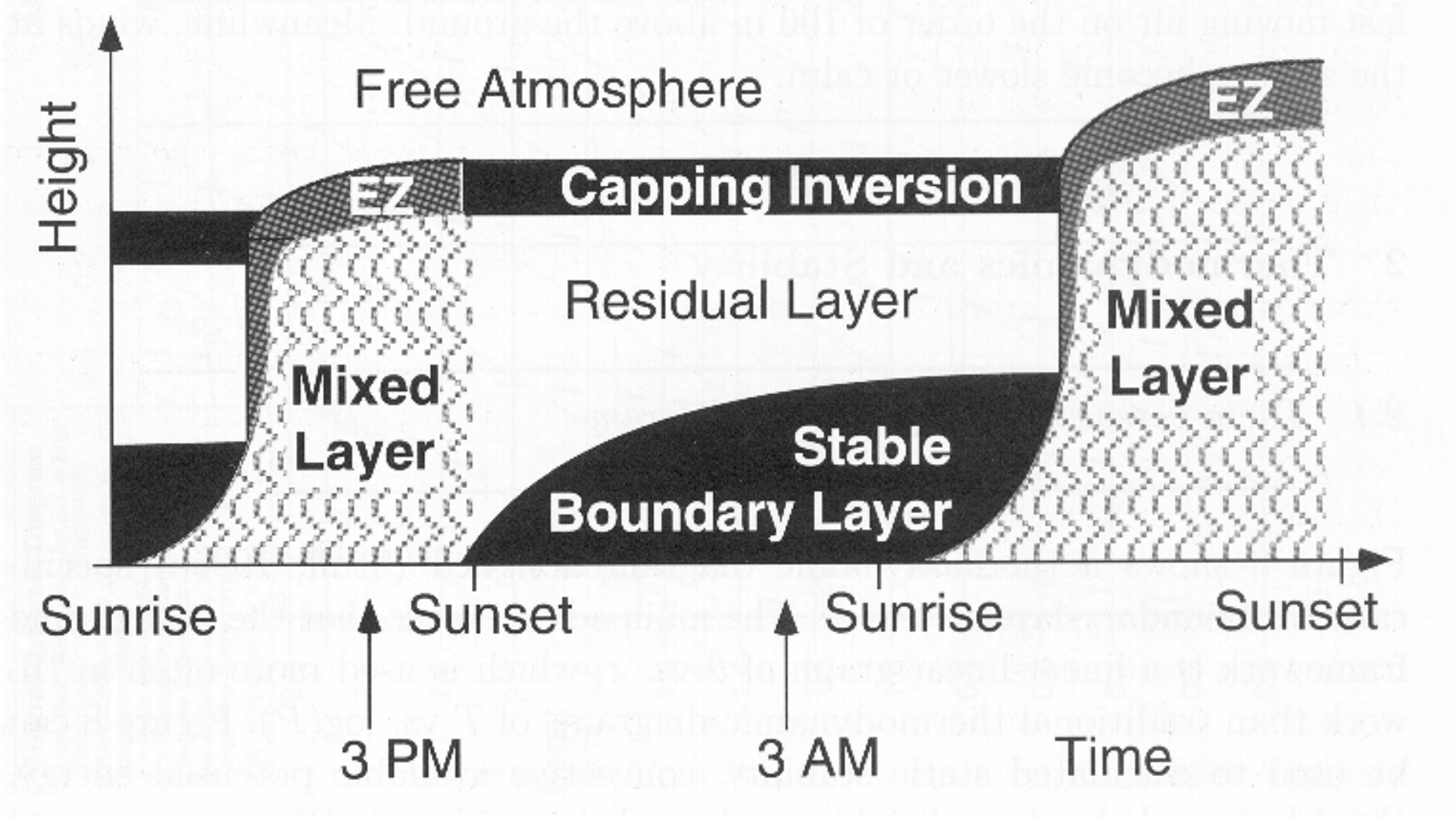

Comparing structural features of CBL and SBL

after John Wyngaard and Roland Stull

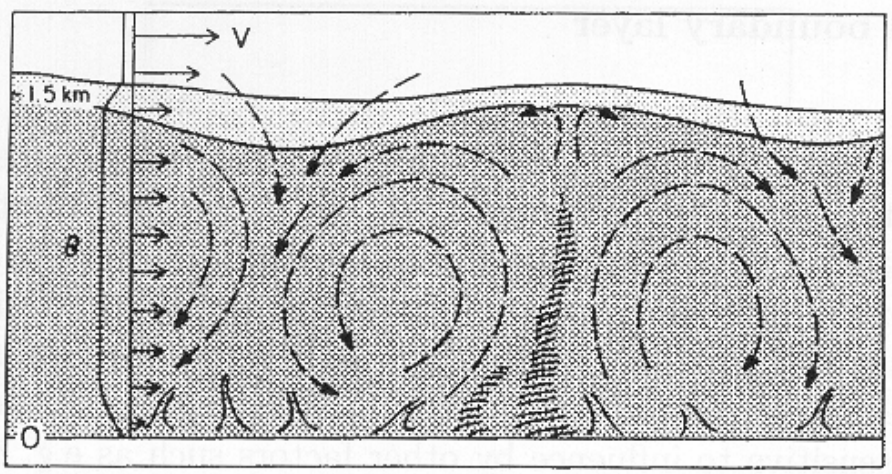

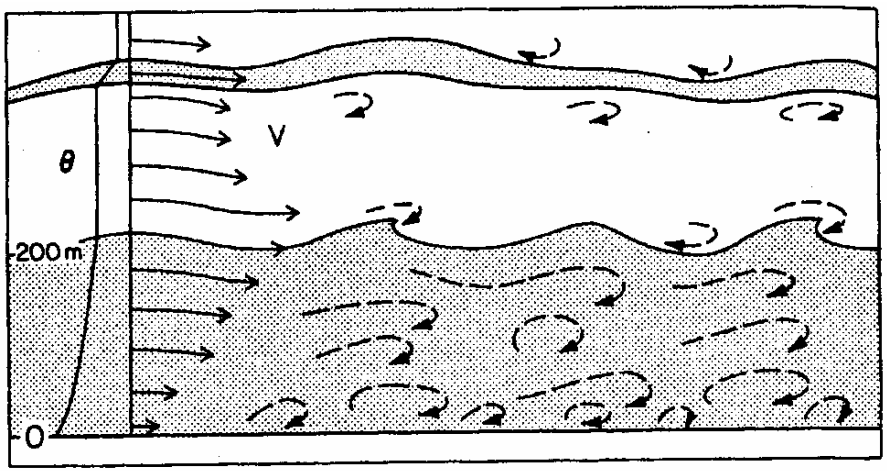

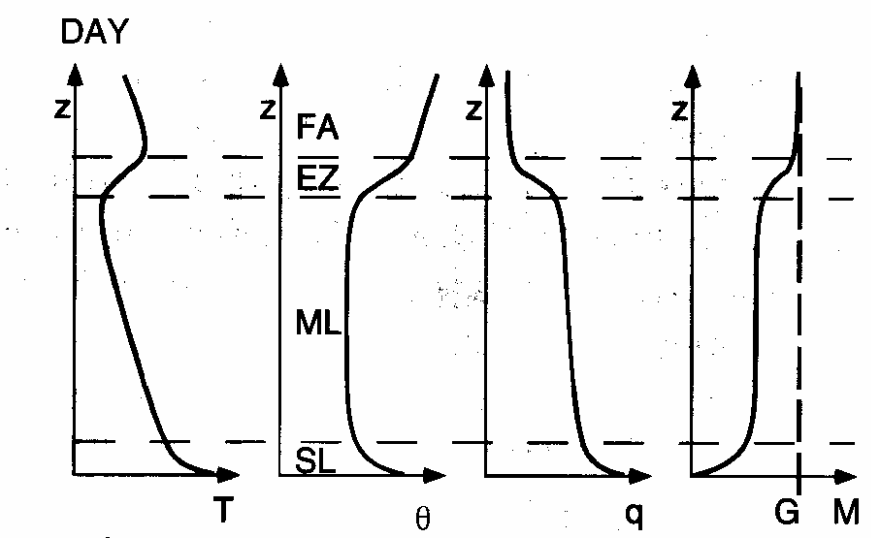

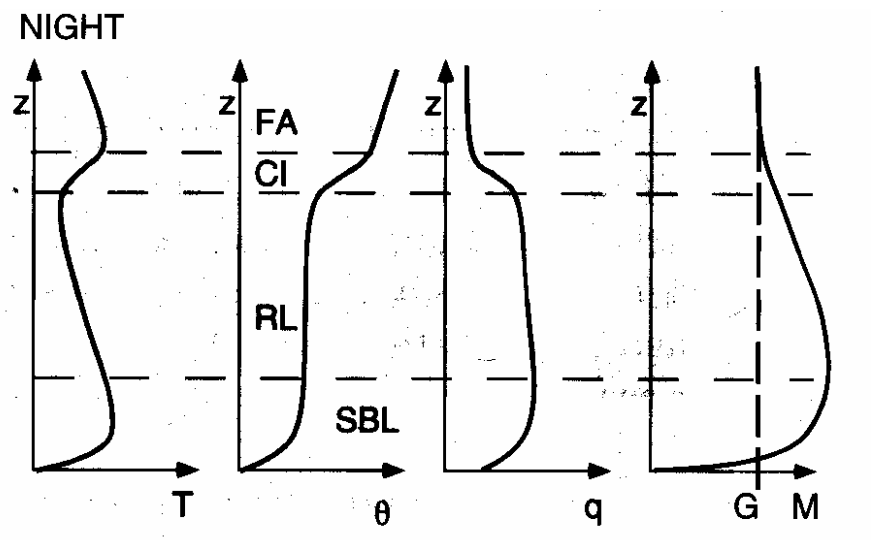

CBL (daytime)

SBL (nighttime)

Numerically simulated SBL: mean flow profiles

from LES intercomparison study by Beare et al. (*BLM*, 2006)

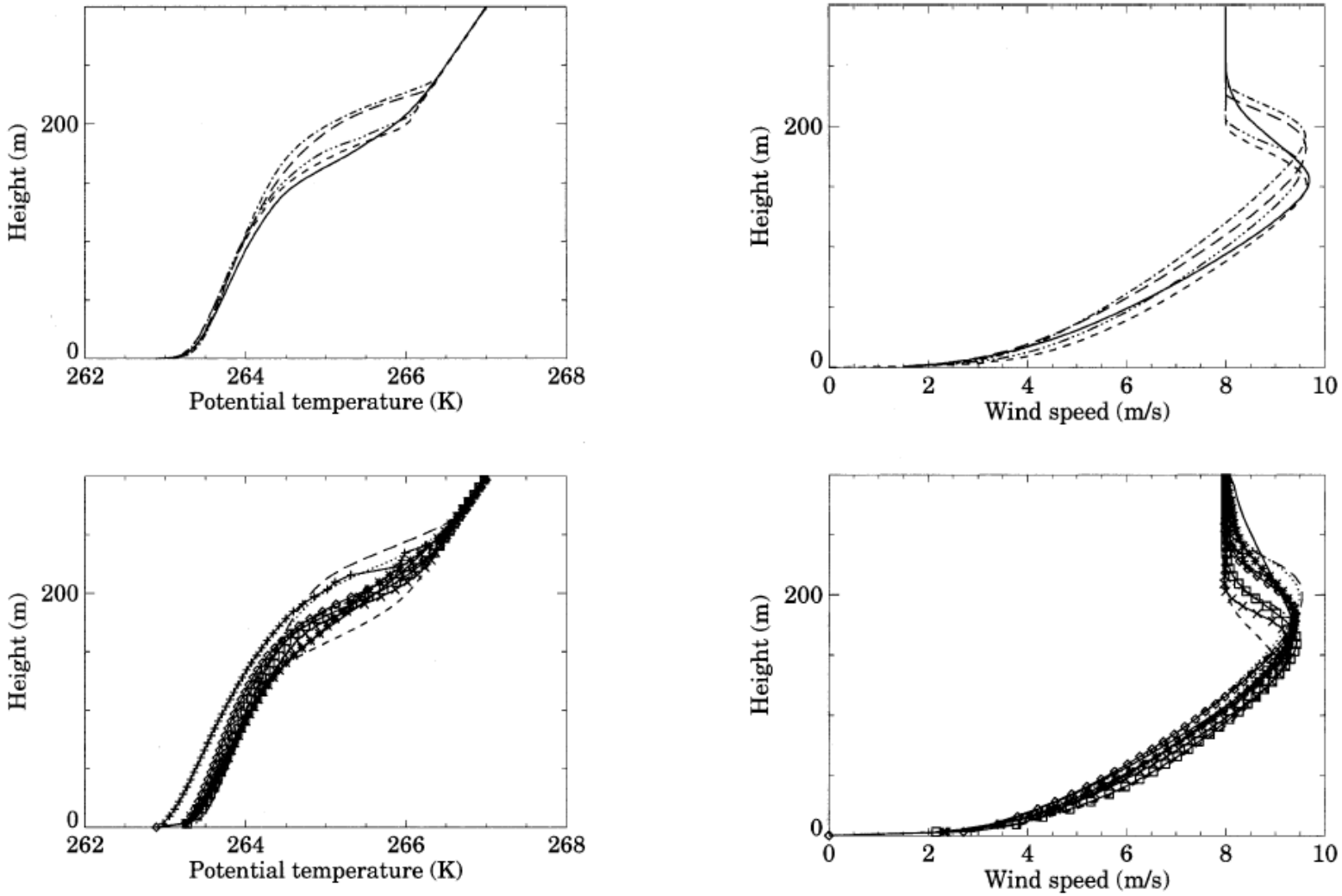

Top: with 2-m resolution. Bottom: with 6.25-m resolution.

Numerically simulated SBL: turbulent fluxes

from LES intercomparison study by Beare et al. (*BLM*, 2006)

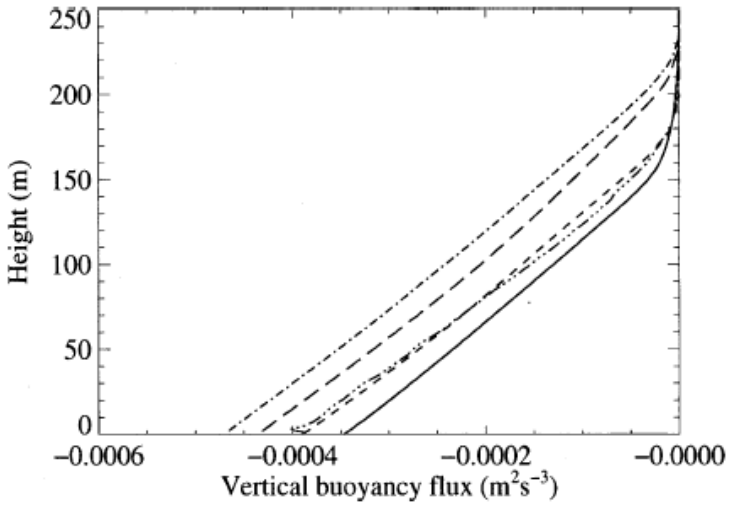

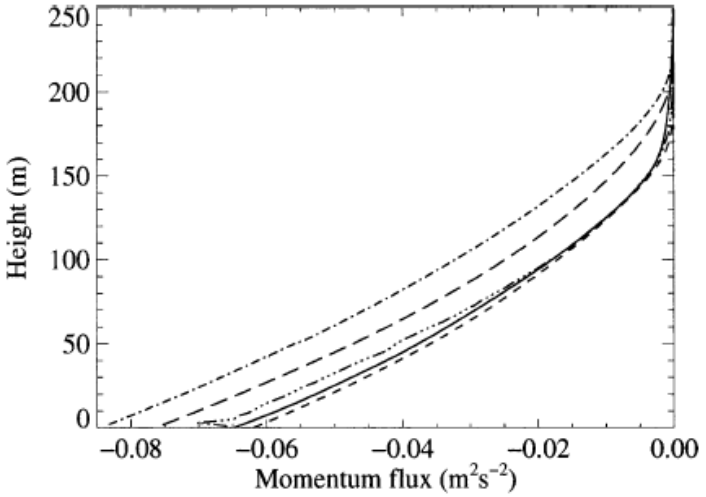

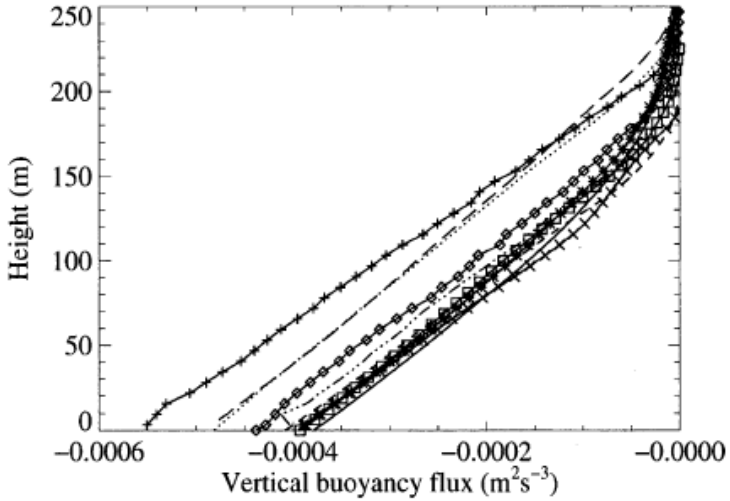

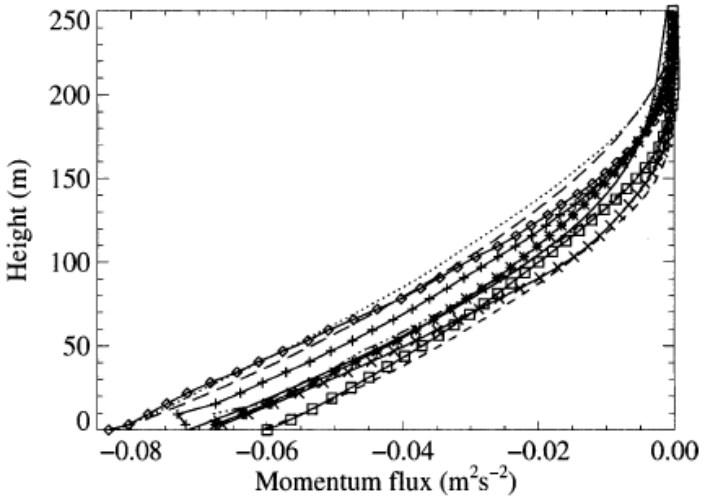

Top: with 2-m resolution. Bottom: with 6.25-m resolution.

Typical setups for wind tunnel modeling of SBL flows

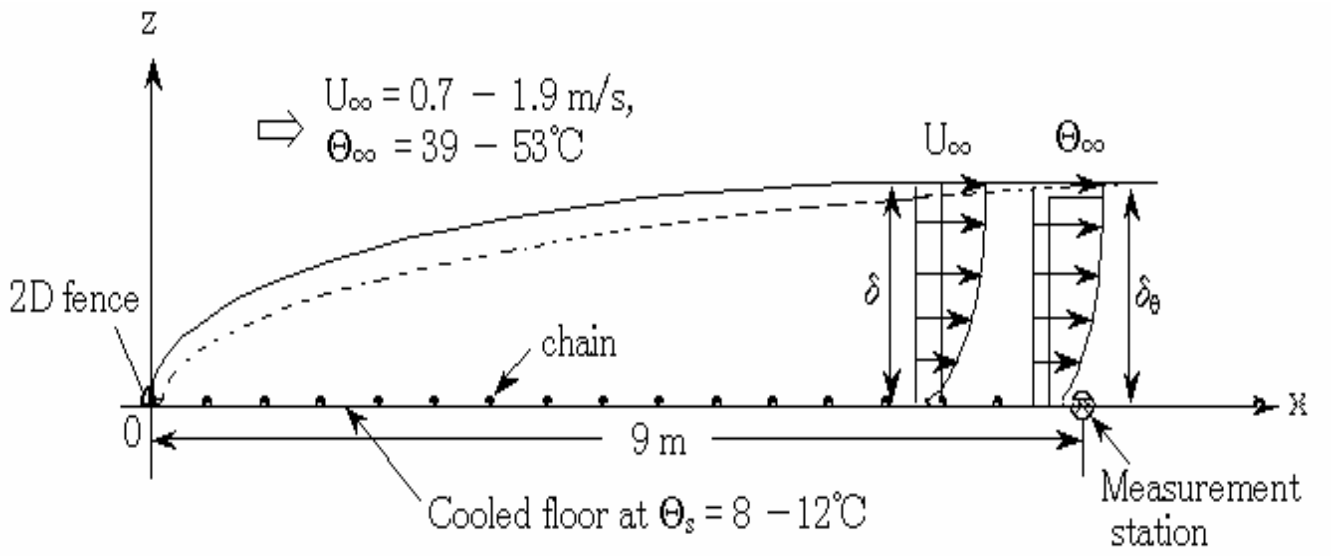

With θ_∞=const

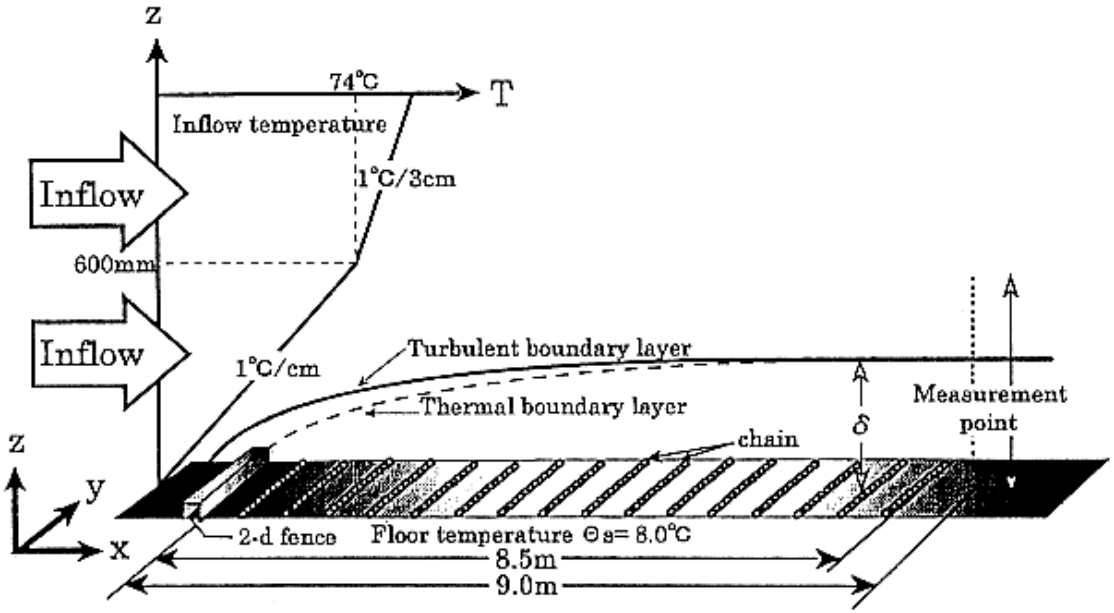

With preshaped θ profile

Stratified wind tunnel of Kiushu University (Japan)

Courtesy of Yuji Ohya

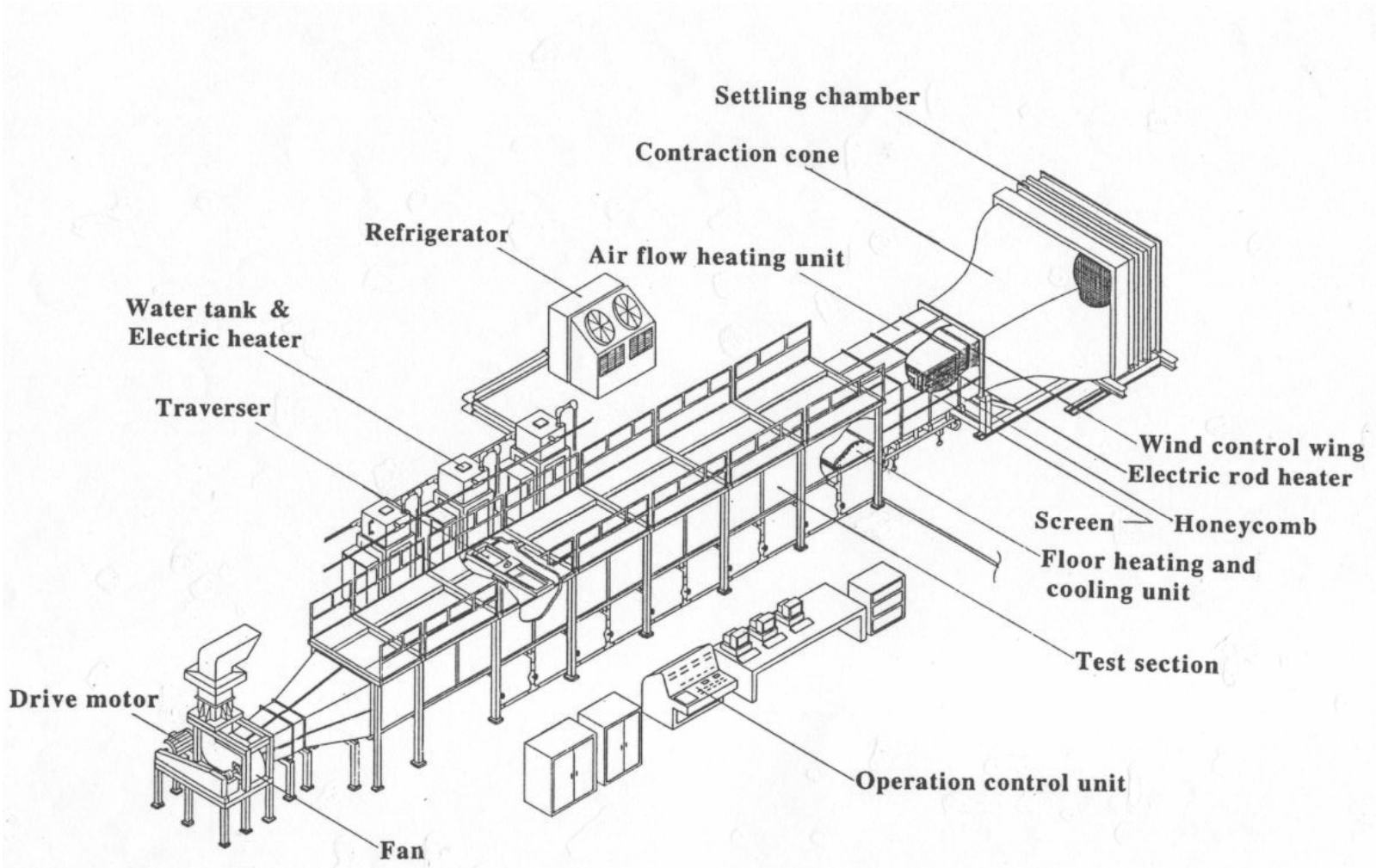

Bird's Eye View of Thermal Stratification Wind Tunnel

Thermal wind tunnel of the University of Minnesota

Courtesy of Fernando Porté-Agel

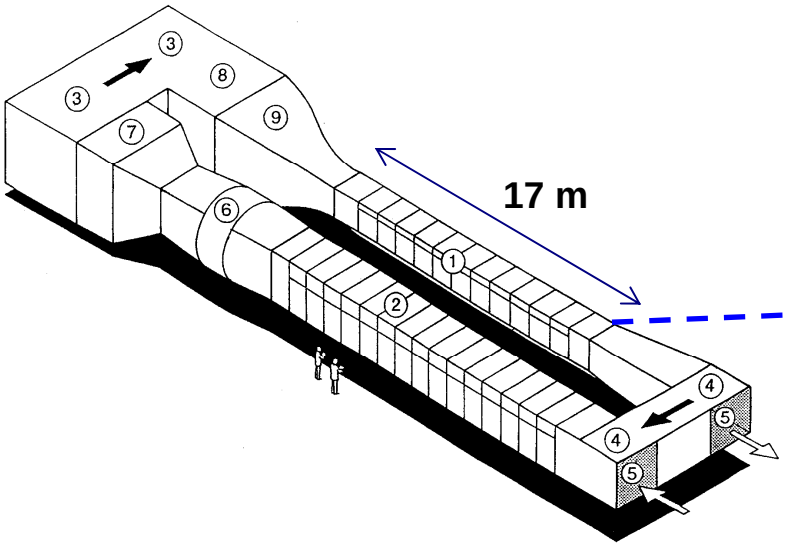

Test section: 17 m x 1.7 m x 1.7 m

Plan Length		37.5 m
Main Test Section	Area	$1.7 \times 1.7 m^2$
	Wind Speed	2-45 m/s
	Contraction Ratio	6.6:1
	FreeStream Turb. Intensity	$< 0.3\%$
	Adjustable Roof	1.5-1.7 m
Larger Test Section	Area	$2.4 \times 2.4\ m^2$
	Wind Speed	1-18 m/s
Fan	Diameter	2.4 m
	Max. RPM	900
	Electric Motor	200 hp

- Air temperature control: 5C – 45C
- Floor temperature control: 5C – 45C
- Different sections of the floor can be set to different temperatures in the range 5-45 C

Monin-Obukhov (M-O) similarity in stable surface layer

Turbulence scales: **velocity** $u_* = (-\overline{u'w'})^{1/2}$, **temperature** $\theta_* = -\overline{w'\theta'}/u_*$,

humidity $q_* = -\overline{w'q'}/u_*$, **buoyancy** $b_* = -\overline{w'b'}/u_* = \beta\theta_* + 0.61 g q_*$.

M-O hypothesis and universal functions

$$\frac{\kappa z}{u_*}\frac{\partial u}{\partial z} = \kappa\frac{z}{L}\varphi_m'(z/L) \equiv \varphi_m(\zeta), \qquad \frac{\kappa z}{\theta_*}\frac{\partial \theta}{\partial z} = \kappa\frac{z}{L}\varphi_h'(z/L) \equiv \varphi_h(\zeta),$$

$$\frac{\kappa z}{q_*}\frac{\partial q}{\partial z} = \kappa\frac{z}{L}\varphi_q'(z/L) \equiv \varphi_q(\zeta), \qquad \frac{\kappa z}{b_*}\frac{\partial b}{\partial z} = \kappa\frac{z}{L}\varphi_b'(z/L) \equiv \varphi_b(\zeta),$$

$$L = -\frac{(-\overline{u'w'})^{3/2}}{\kappa\overline{w'b'}} = \frac{u_*^{\,2}}{\kappa b_*} \text{ (M-O length)}, \quad \zeta = z/L, \quad \varphi_h(\zeta) \approx \varphi_q(\zeta) \approx \varphi_b(\zeta)$$

Approximations of similarity functions

Businger *et al.*: $\varphi_m(\zeta) = 1 + 4.7\zeta$, $\varphi_h(\zeta) = 0.74 + 4.7\zeta$, $\kappa = 0.35$

Dyer *et al.*: $\varphi_m(\zeta) = 1 + 5\zeta$, $\varphi_h(z/L) = 1 + 5\zeta$, $\kappa = 0.4$ (originally, 0.41)

Turbulent diffusivities and Richardson numbers

Combining $k(\partial u/\partial z)=u_*^2$ with $\dfrac{\kappa z}{u_*}\dfrac{\partial u}{\partial z}=\varphi_m(\zeta)$, **and**

$k_h(\partial\theta/\partial z)=u_*\theta_*$ with $\dfrac{\kappa z}{\theta_*}\dfrac{\partial\theta}{\partial z}=\varphi_h(\zeta)$, **provides turbulent diffusivities,**

$$k(z)=\frac{\kappa u_* z}{\varphi_m(\zeta)}=\kappa u_* L\frac{\zeta}{\varphi_m(\zeta)},\qquad k_h(z)=\frac{\kappa u_* z}{\varphi_h(\zeta)}=\kappa u_* L\frac{\zeta}{\varphi_h(\zeta)}.$$

Richardson numbers

$$\mathrm{Ri}_f=\frac{\overline{w'b'}}{\overline{u'w'}(\partial u/\partial z)}$$ **flux Richardson number,**

$$\mathrm{Ri}=\frac{\partial b/\partial z}{(\partial u/\partial z)^2}$$ **gradient Richardson number,**

with $\mathrm{Ri}_f=(k_h/k)\mathrm{Ri}=\mathrm{Ri}/\mathrm{Pr}_t$, characterize **ratio of buoyancy to shear** contributions to the TKE production.

Relationships between different stability parameters

In terms of Dyer's functions, with $\zeta = z/L \geq 0$:

$$\mathrm{Ri} = \mathrm{Ri}_f = \zeta/(1+5\zeta) \geq 0.$$

Inverse relationship, $\zeta = \mathrm{Ri}/(1-5\mathrm{Ri})$, yields **Ri=0.2** as a **critical Ri value**. It corresponds to the infinitely large positive ζ or, for a given z, infinitesimal positive L that is the case of extreme stability when turbulence cannot exist.

Also, for $\zeta = z/L \geq 0$:

$$k(z) = k_h(z) = \kappa u_* z(1-5\mathrm{Ri}).$$

Other useful relationships between stability parameters and universal functions:

$$\mathrm{Pr}_t = \varphi_h/\varphi_m = k/k_h = \mathrm{Ri}/\mathrm{Ri}_f,$$

$$\mathrm{Ri} = \frac{\varphi_h}{\varphi_m^{\,2}}\frac{z}{L} = \frac{\mathrm{Pr}_t}{\varphi_m}\zeta, \qquad \mathrm{Ri}_f = \frac{1}{\varphi_m}\frac{z}{L} = \frac{\mathrm{Pr}_t}{\varphi_h}\zeta.$$

SBL flow in experiments of Ohya and Uchida (*BLM*, 2003)

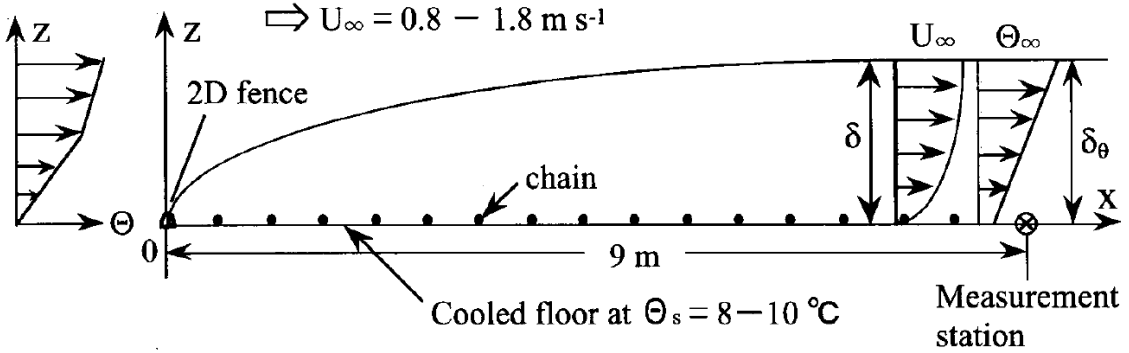

Figure 1. Experimental arrangement.

TABLE I

Experimental conditions of neutral (case N1) and stable boundary boundary layers (cases S1–S3).

Exp. case	N1	S1	S2	S3
U_∞ (m s^{-1})	1.76	1.57	1.11	0.86
Re_δ	52800	43500	30700	29300
Ri_δ	–	0.28	0.56	1.38
δ (m)	0.45	0.45	0.45	0.55
$\Delta\theta$ (°C)	–	47.4	47.0	57.9
u_*/U_∞	0.054	0.032	0.028	–
L (m)	∞	0.34	0.12	–
Symbol	●	□	Δ	○

$$\mathrm{Re}_\delta = \frac{U_\infty \delta}{\nu}, \qquad \mathrm{Ri}_\delta = \frac{\beta(\theta_\infty - \theta_s)\delta}{U_\infty^{\,2}}$$

Flow regime changes with increasing stability

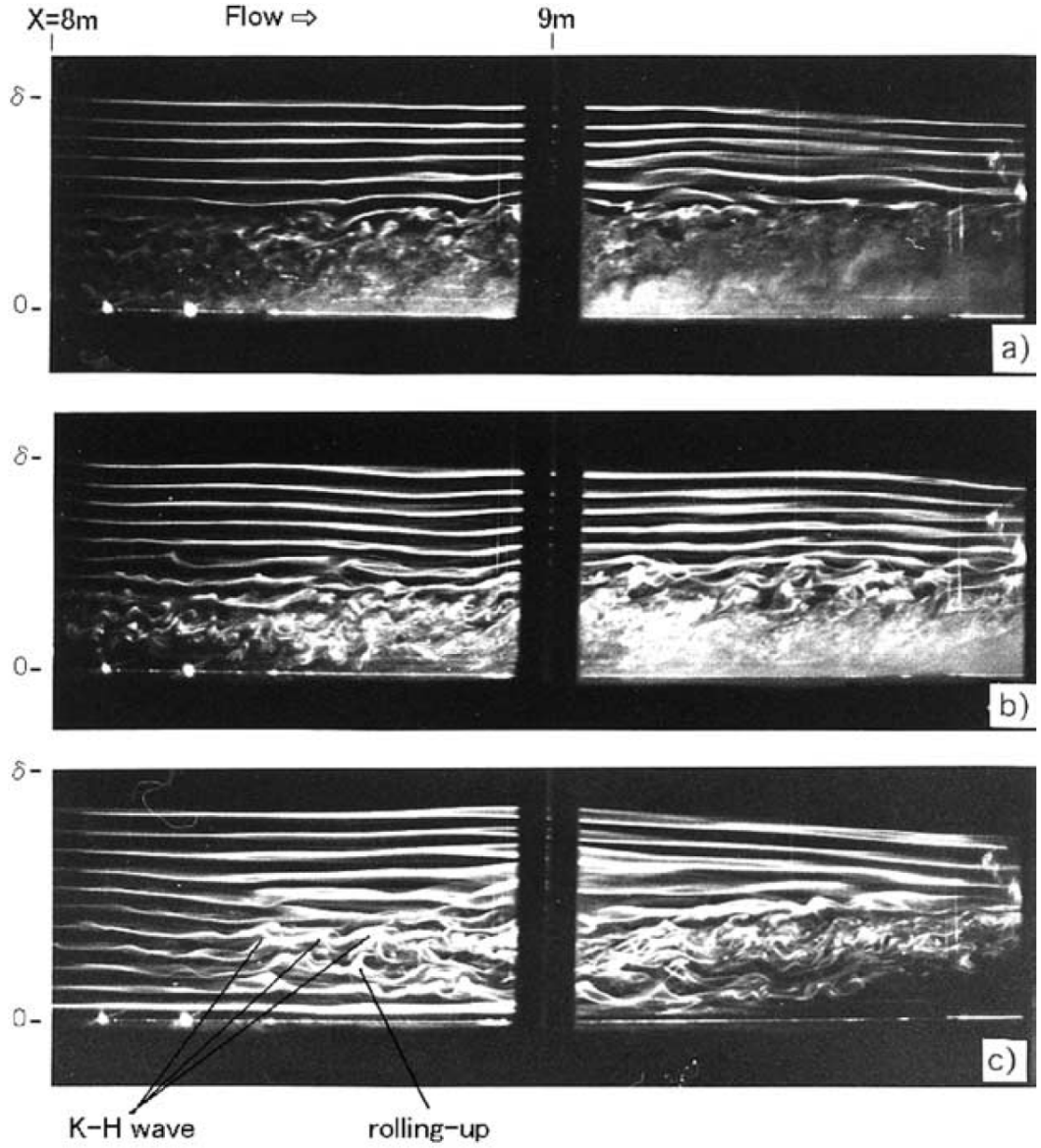

Figure 7. Flow visualization of stable boundary layers for cases S1–S3. Side view at $x = 8$–10 m. Flow is left to right: (a) Very weak stability (case S1), (b) weak stability (case S2), (c) strong stability (case S3), the arrows indicate K–H waves.

Mean flow parameters in SBL of Ohya and Uchida

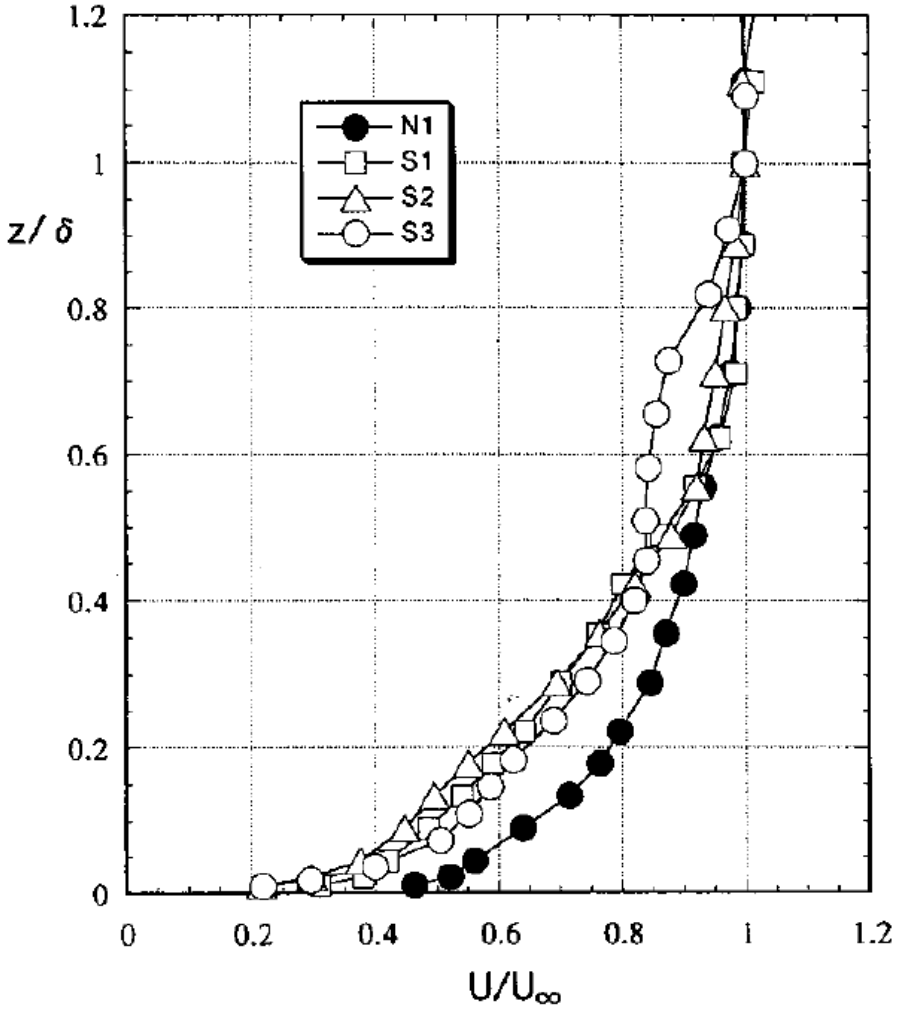

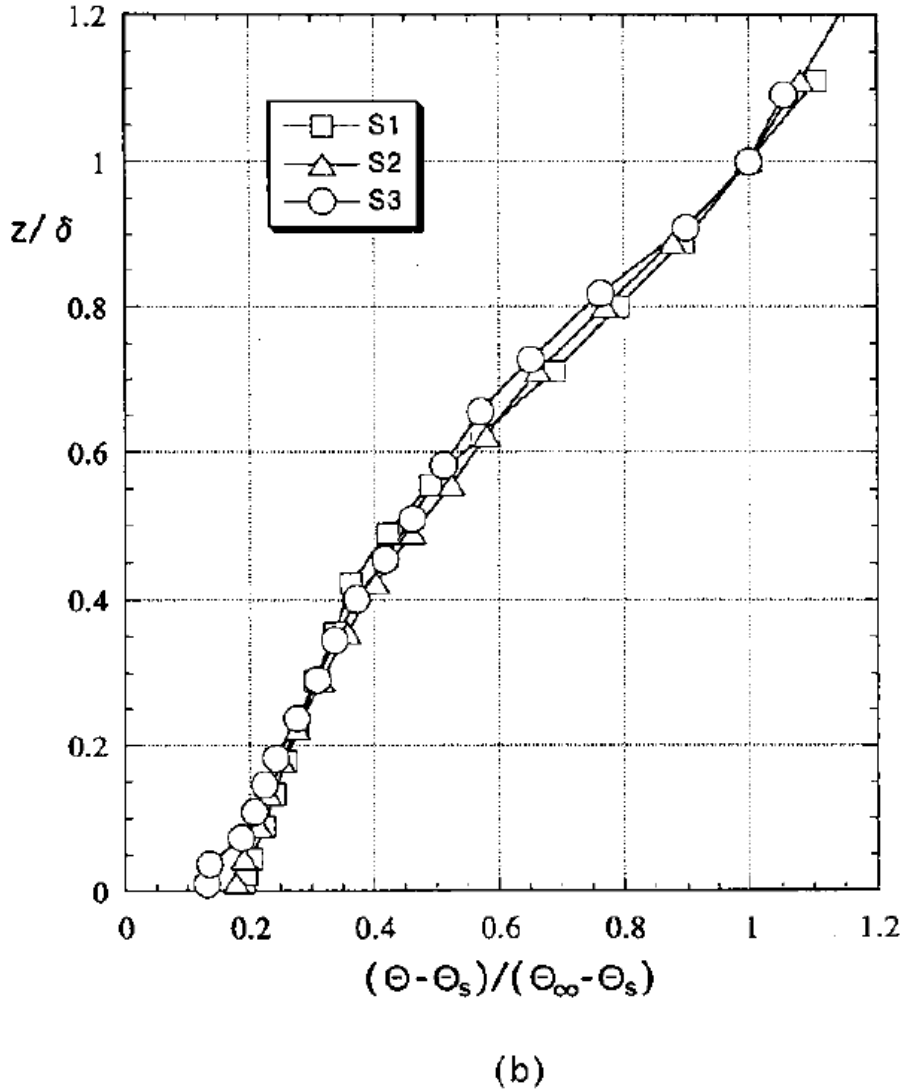

Figure 2. Vertical profiles of the mean velocity and temperature: (a) Streamwise velocity U, (b) temperature Θ.

Turbulence statistics in SBL of Ohya and Uchida

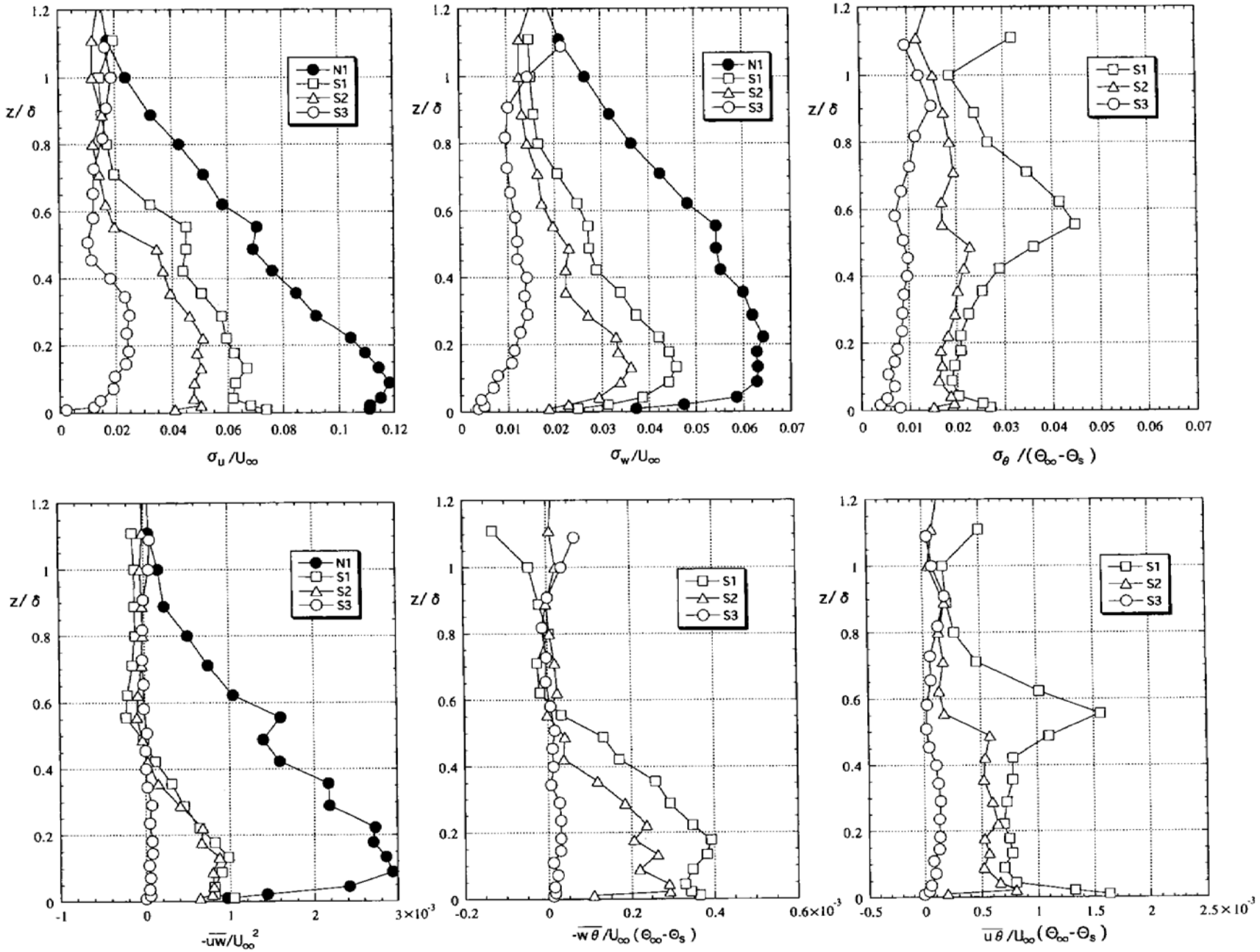

Gradient Ri numbers in SBL of Ohya and Uchida

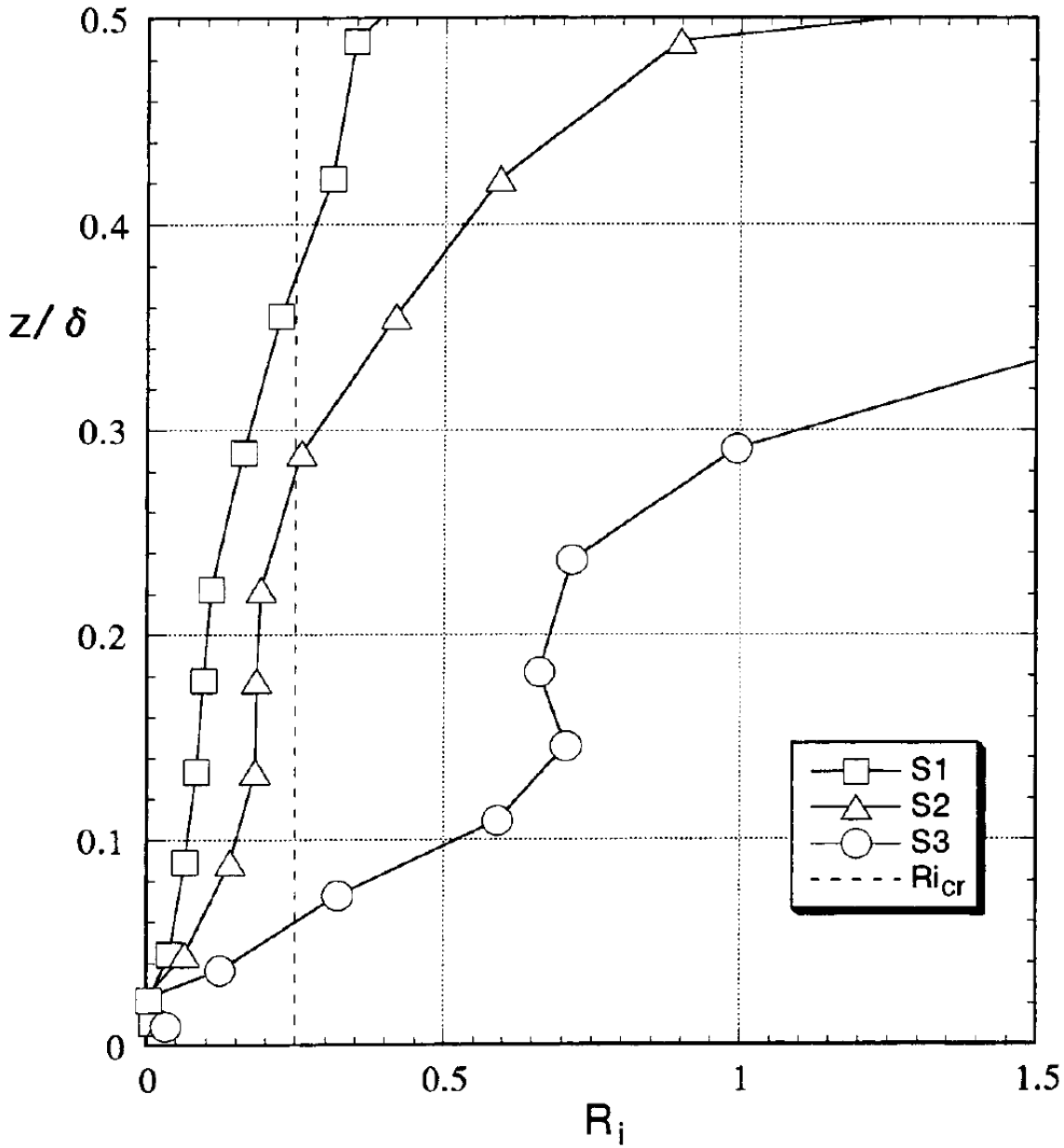

Figure 5. Vertical profiles of the local gradient Richardson number Ri.

Turbulence statistics as functions of Ri in SBL of Ohya and Uchida

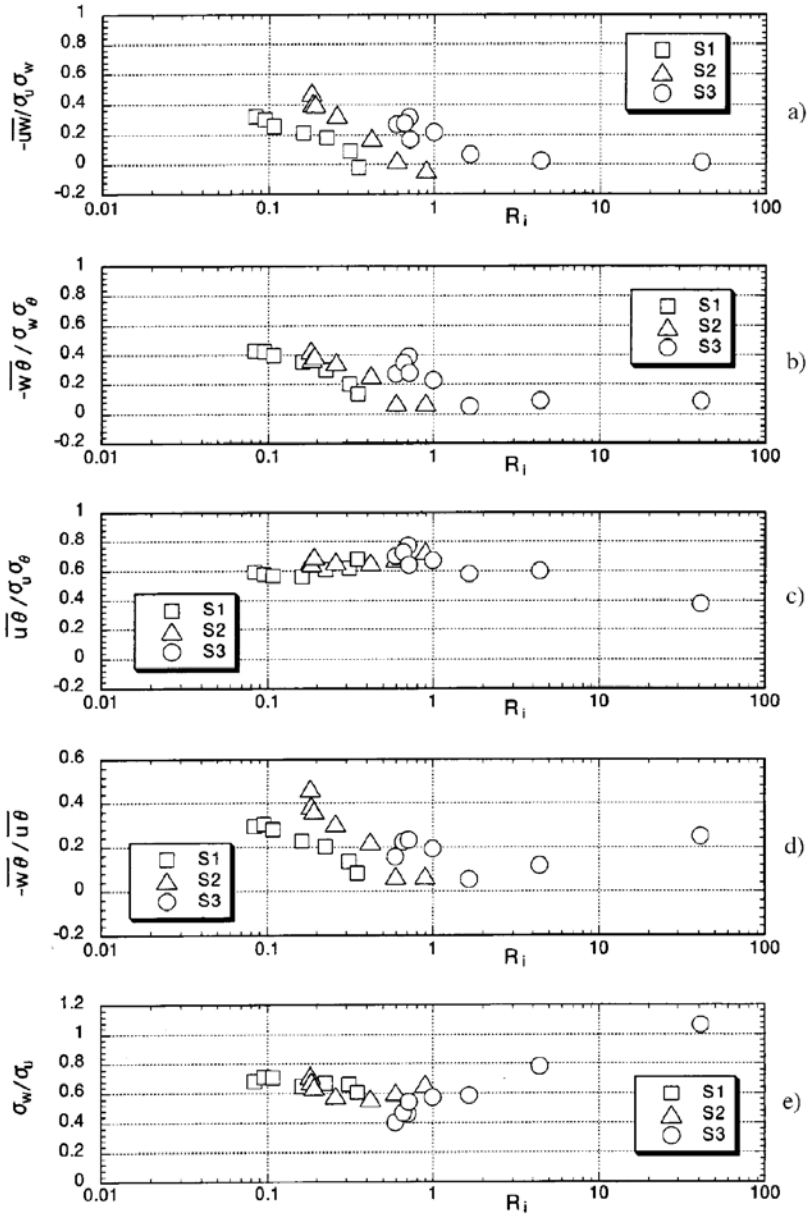

Figure 6. Correlation of normalized turbulence quantities with local gradient Richardson number Ri: (a) Vertical momentum flux, (b) vertical heat flux, (c) horizontal heat flux, (d) ratio of vertical and horizontal heat fluxes, (e) ratio of turbulence intensities.

Wind tunnel models of BL flows within/above …

URBAN →  **and**

FOREST →  **canopies**

Main structural features of urban canopy layer

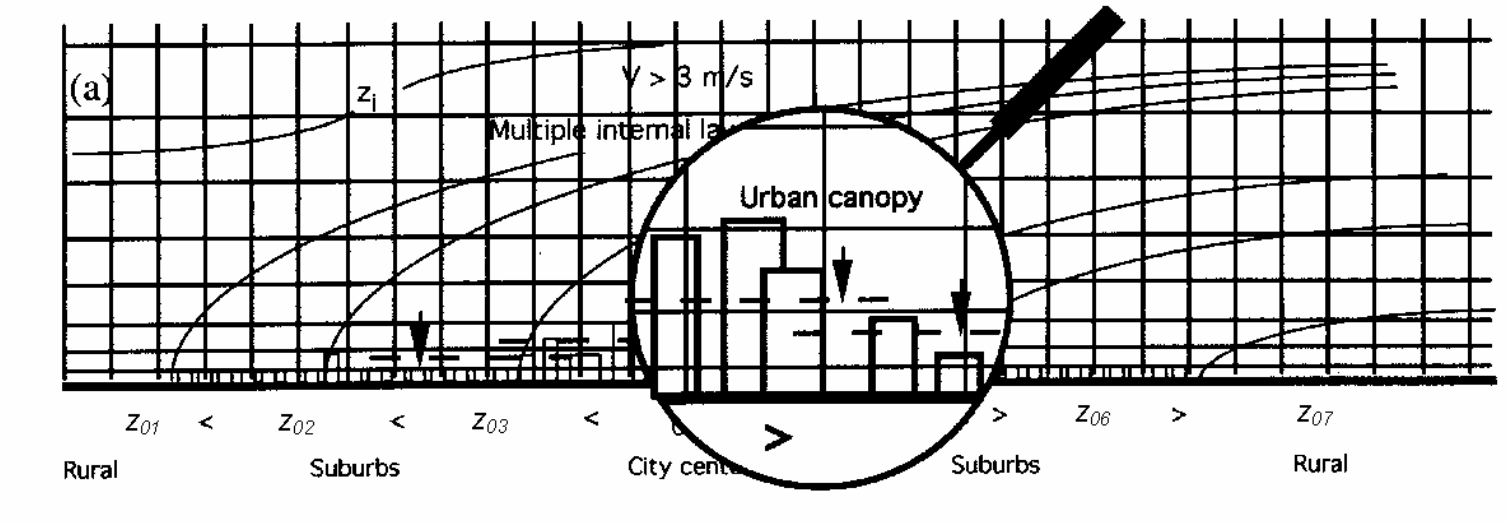

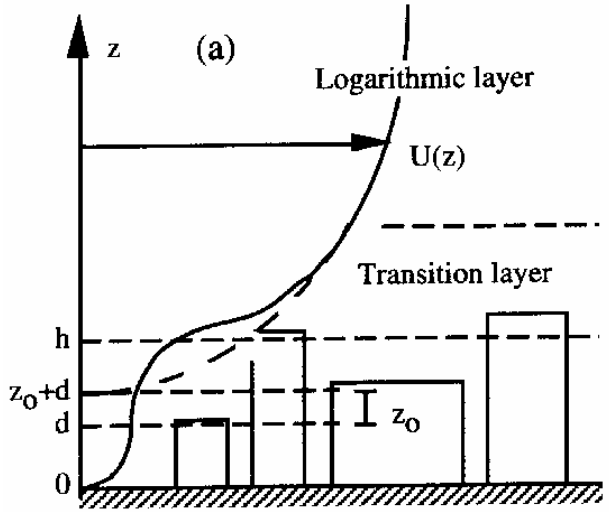

From Mestayer, P. G., and S. Anquetin, 1995: Climatology of cities. In *Diffusion and Transport of Pollutants in Atmospheric Mesoscale Flows*, A. Gyr and F.-S. Rys (Eds.), Kluwer.

Characteristic urban canopy: Nantes, France

after Petra Kastner-Klein et al. (2000-2004)

Plan

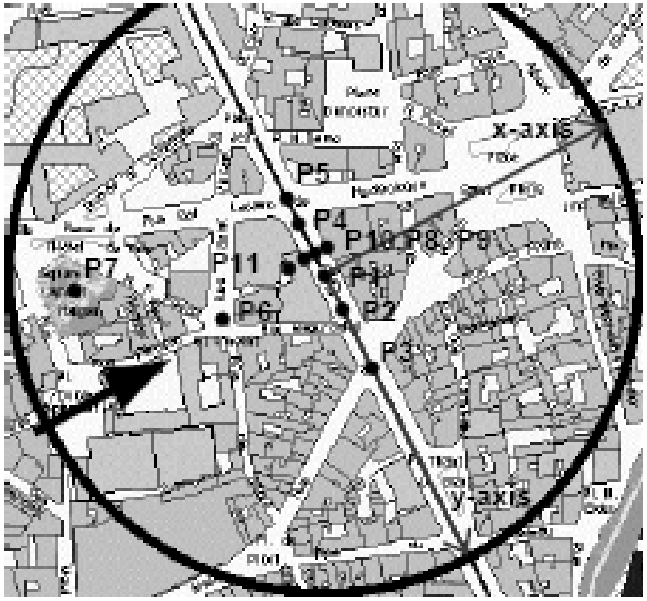

WT model

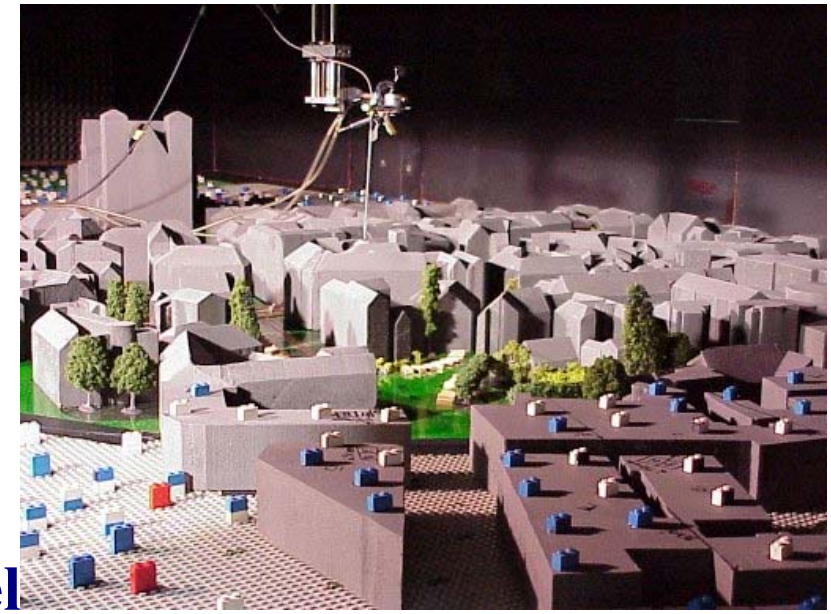

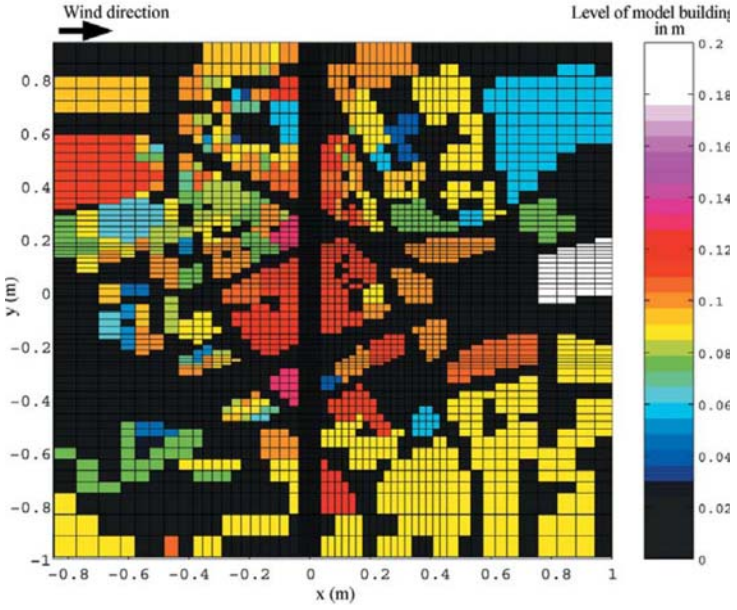

Building height distribution in the model

Measurement locations and flow parameters in Nantes model

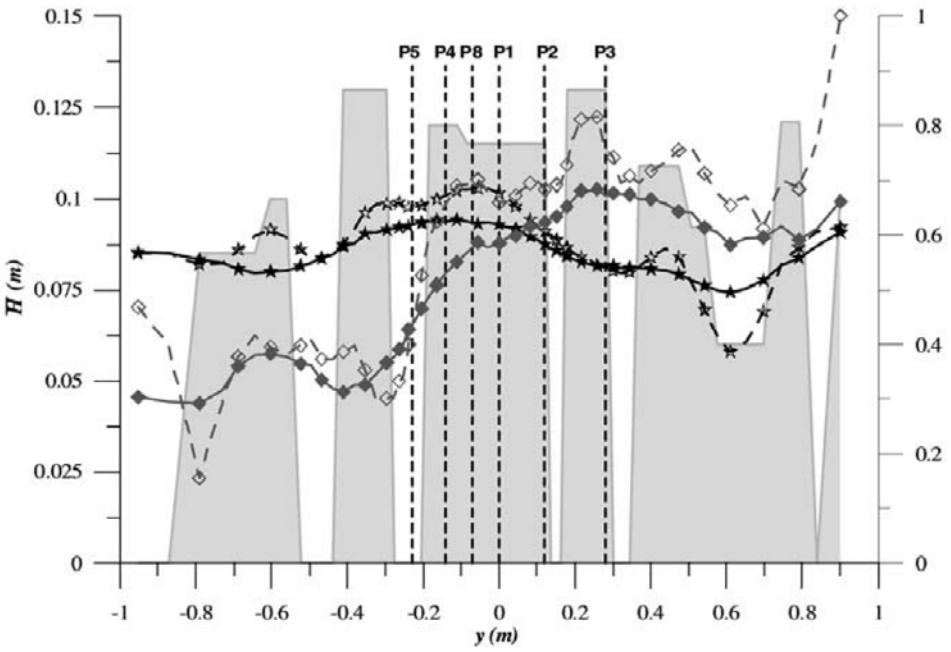

TABLE II

Description of sampling point locations and corresponding wind-profile parameters determined by a morphometric method (d_{0m}) and fitting the measured mean wind profiles against the log law (z_{0p}, u_{*p}).

	x (m)	y (m)	d_{0m} (mm)	z_{0p} (mm)	u_{*p} (m s^{-1})	Symbol
P1	0.0	0.0	96.00	6.87	0.70	☆
P2	0.0	0.12	88.00	5.18	0.66	×
P3	0.0	0.28	82.00	3.09	0.58	×
P4	0.0	−0.14	99.00	6.69	0.69	○
P5	0.0	−0.23	87.00	15.36	0.91	○
P6	−0.33	0.0	90.00	6.10	0.67	☆
P7	−0.66	−0.23	75.00	4.48	0.64	★
P8	0.0	−0.7	101.00	5.19	0.65	◊
P9	0.02	−0.07	101.00	5.29	0.65	▽
P10	−0.02	−0.07	101.00	5.30	0.65	△
P11	−0.08	−0.07	101.00	3.99	0.61	▲
REF	−1.80	0.0	0.2	0.86	0.42	solid line

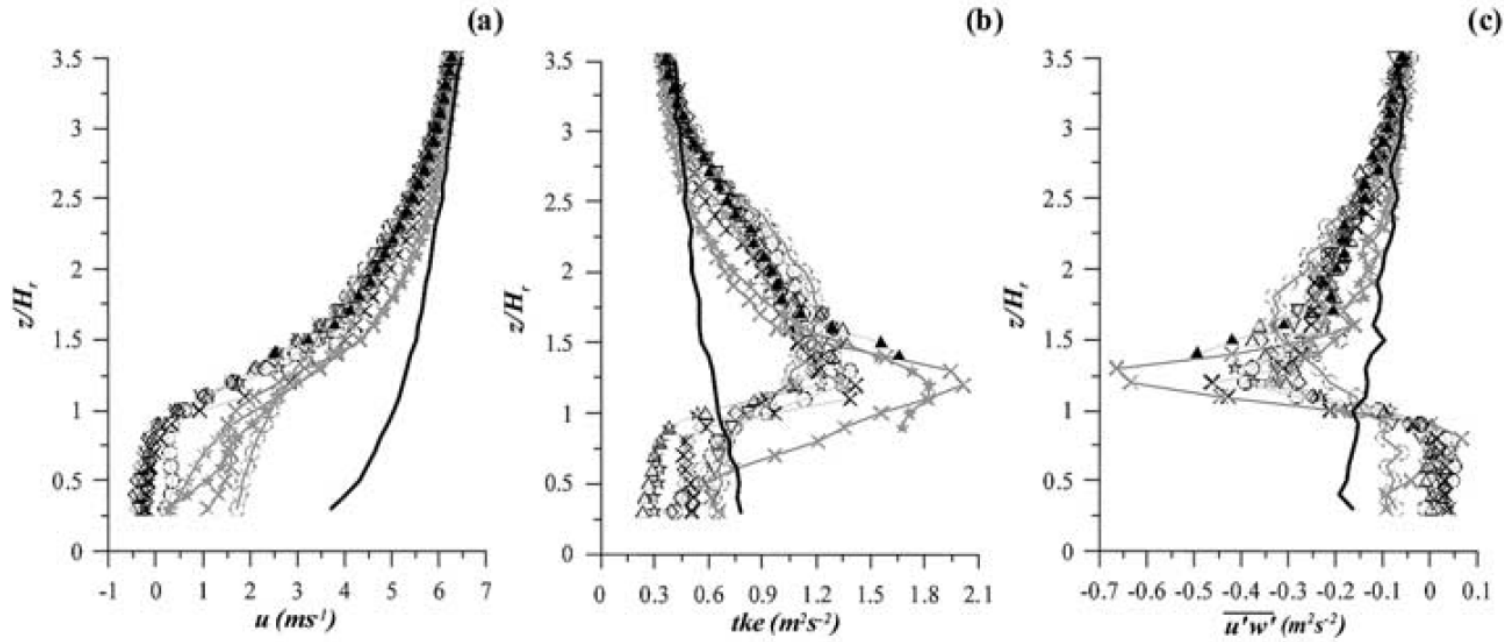

Normalized momentum flux in Nantes model

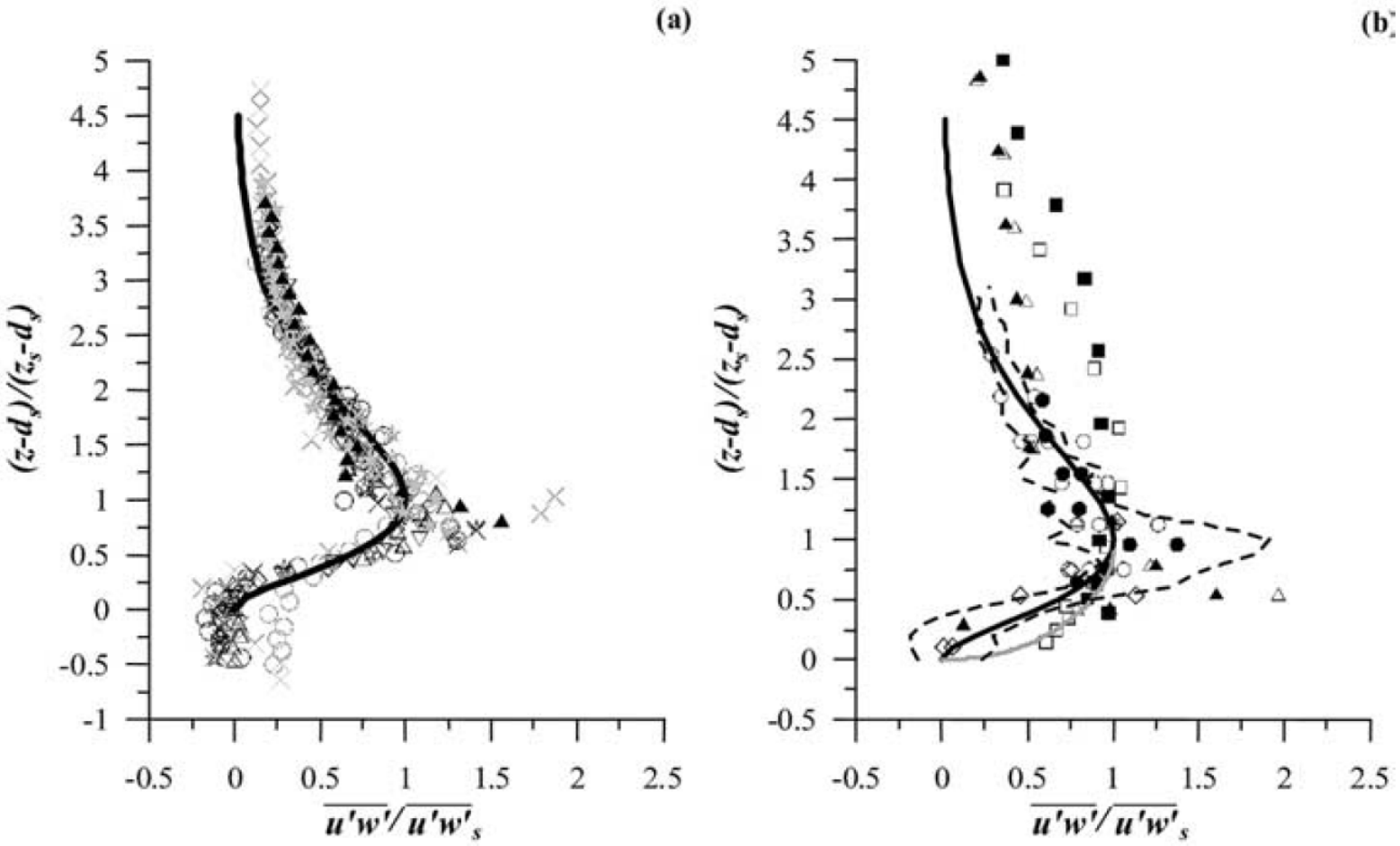

Figure 10. (a) Scaling of wind-tunnel shear stress profiles measured in the Nantes study (symbols according to Table II) and (b) comparison of proposed shear-stress parameterizations according to Equations (4) and (10) with full-scale and wind-tunnel data published in the literature (Rotach (1993a): ◊; Louka (1999), smooth-rough case: ○, rough-rough case: ●; Oikawa and Meng (1995): ★, Rafailidis (1997), aspect ratio $S/H = 1$ with flat roofs: ■, aspect ratio $S/H = 0.5$ with flat roofs: □, aspect ratio $S/H = 1$ with slanted roofs: ▲, aspect ratio $S/H = 0.5$ with slanted roofs: △. Black line: Equation (10), grey line: Equation (4), dashed lines: scatter range of RdS profiles shown

Normalized mean velocity profile in Nantes model

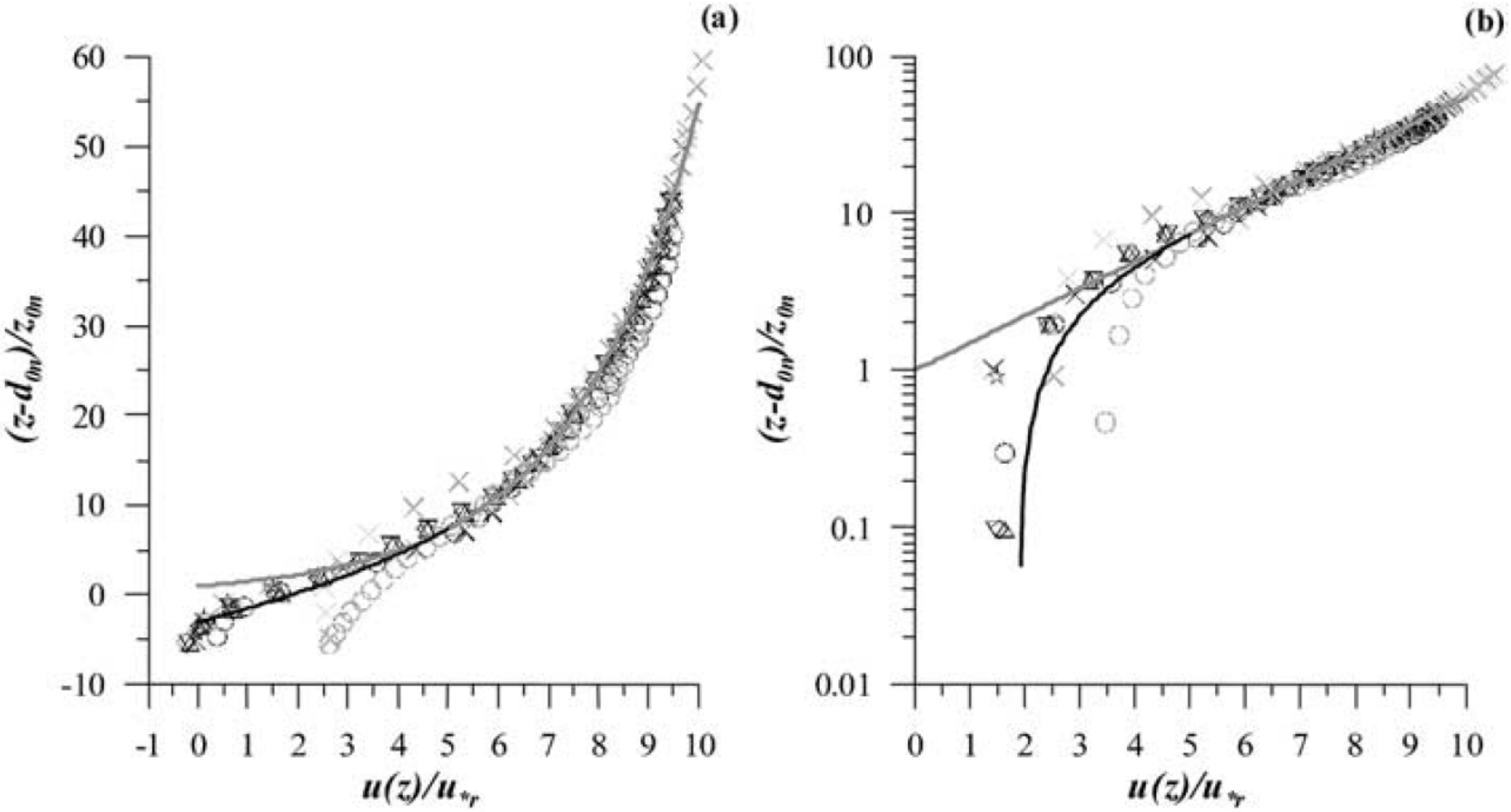

Figure 12. Comparison of the measured mean wind profiles with the log-law profile (Equation (1), grey line) and a profile for the RSL that is based on a local-scaling approach (Equation (24), black line). The scaling parameters displacement height, d_{0n}, (Equation (15)) and roughness length, z_{0n}, (Equation (16)) are calculated based on the approximated length scales z_{sm} and d_{sm}. The shear-stress velocities, u_{*r}, (Equation (17)) are based on a velocity value, u_{ref}, measured in the reference height, $z_{\mathrm{ref}} = 200$ mm. Plot (b) shows the same as plot (a) but on a semi-log scale.

Modeling flow in/above (under?) forest canopy on a hill

after John Finnigan et al. (2007-2008)

Prototype

Wind tunnel model

Decoupling of flow in the canopy from the outer flow

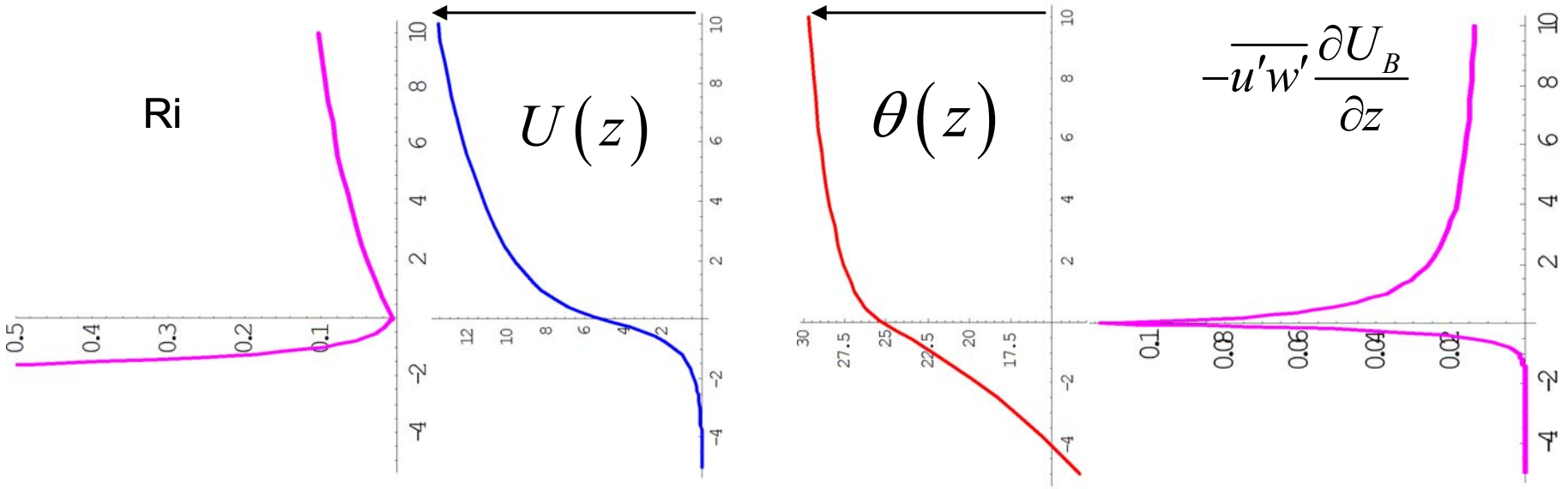

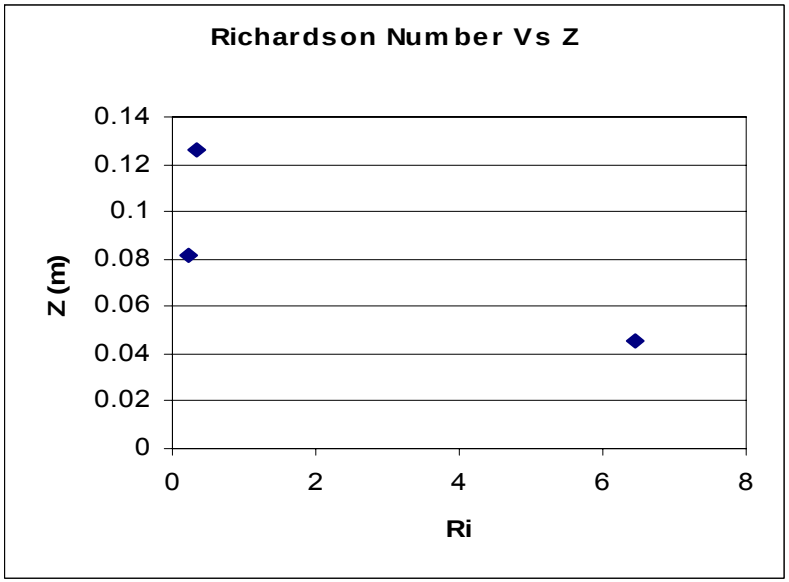

"Heat transfer to canopy elements is via molecular diffusion whereas momentum transfer is effected by pressure. The ratio of their efficiencies is r~O[0.1]"

Harman and Finnigan (2007)

← Wind tunnel data

Thermal effects in forest canopy flow over a hill

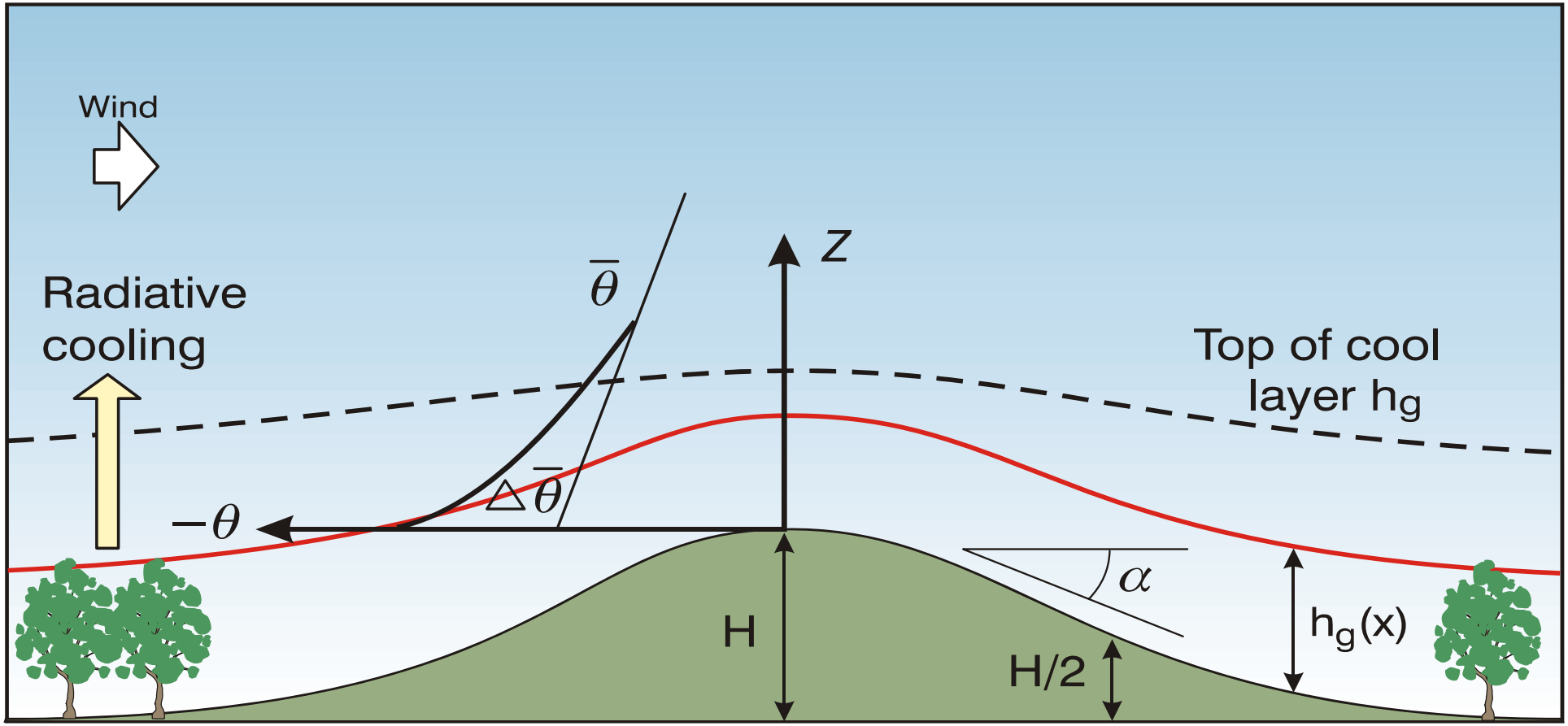

$$\frac{\partial \bar{u}}{\partial t} + U_B.\nabla\bar{u} = -\frac{1}{\rho}\frac{\partial p}{\partial x} + \frac{g}{\Theta_0}\Delta\bar{\theta}\sin\alpha - \frac{\partial\left(\Delta\hat{\theta}h_g\right)}{\partial x}\cos\alpha + \frac{\partial \tau}{\partial z} - 2\left(C_d a\right)U_B\bar{u}$$

Wind tunnel model of forest canopy flow

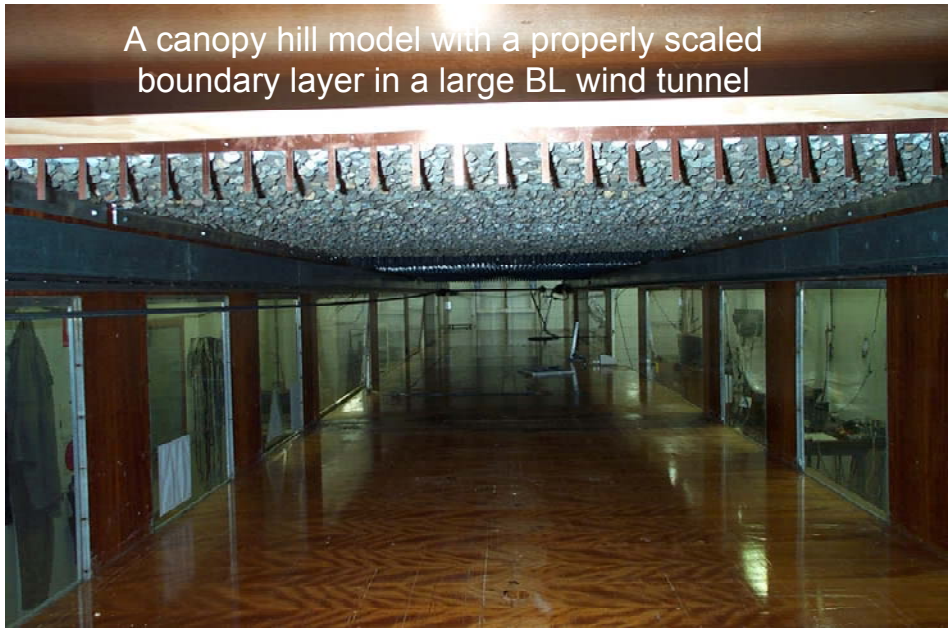

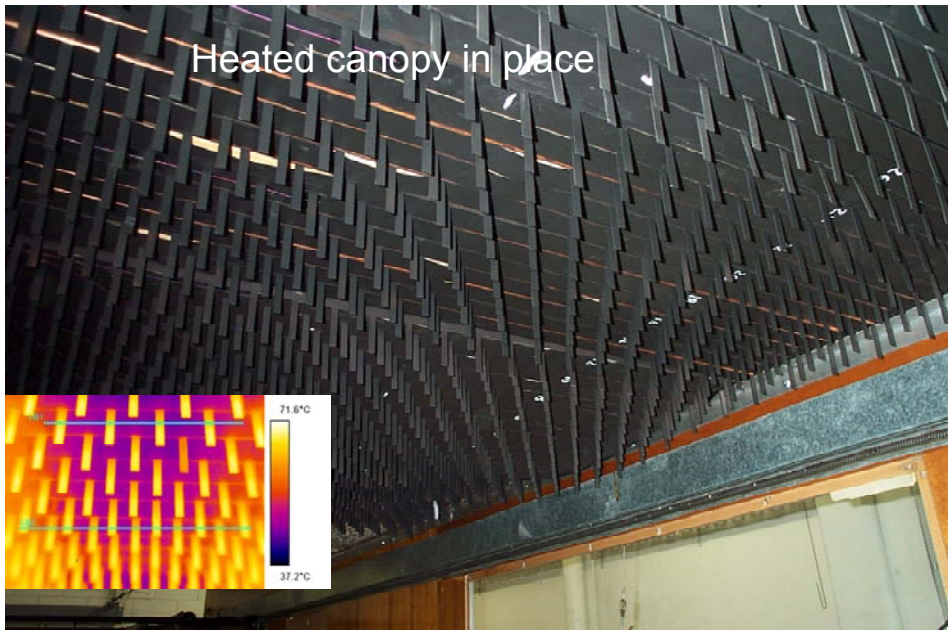

Re-number effects in velocity and momentum flux fields

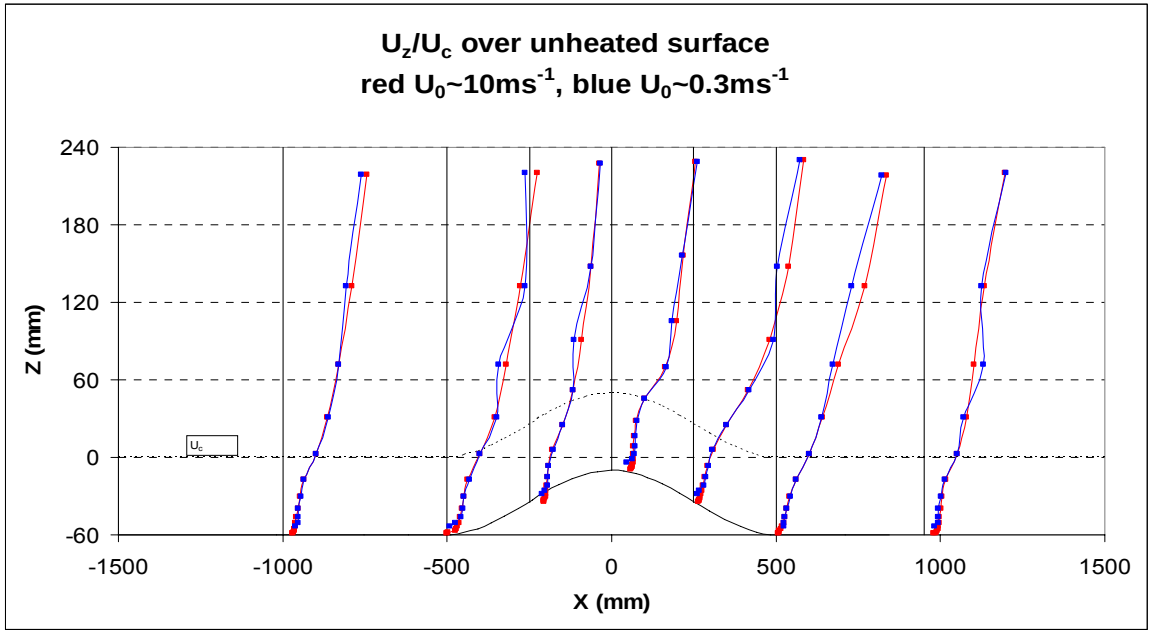

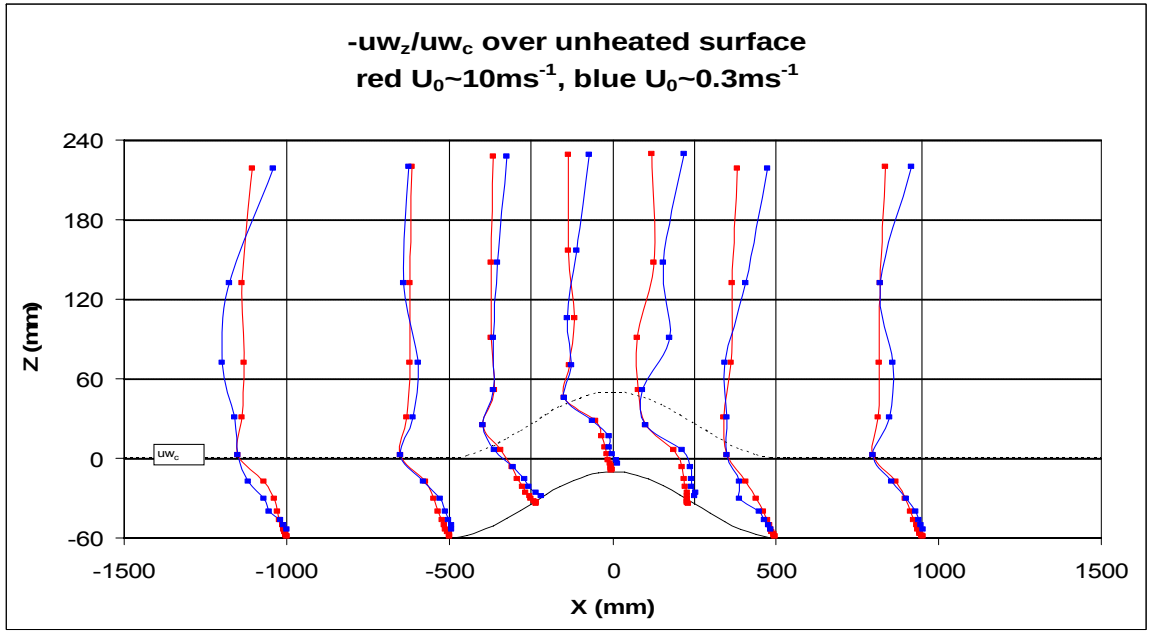

Upwind propagation of thermally induced disturbance

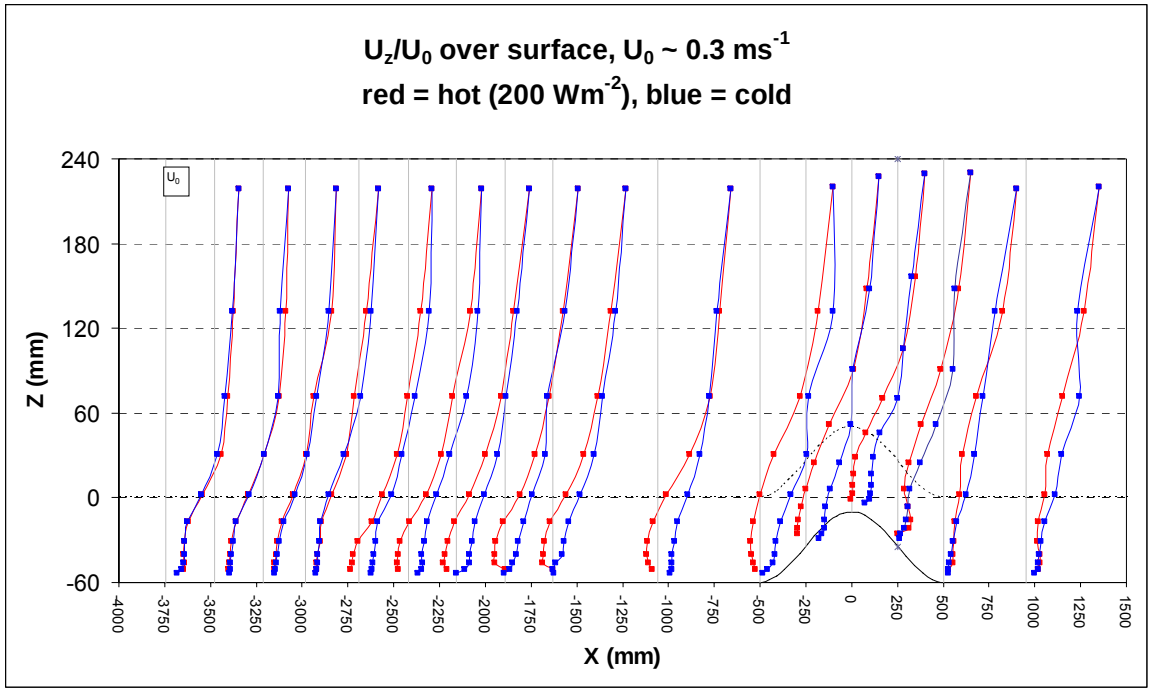

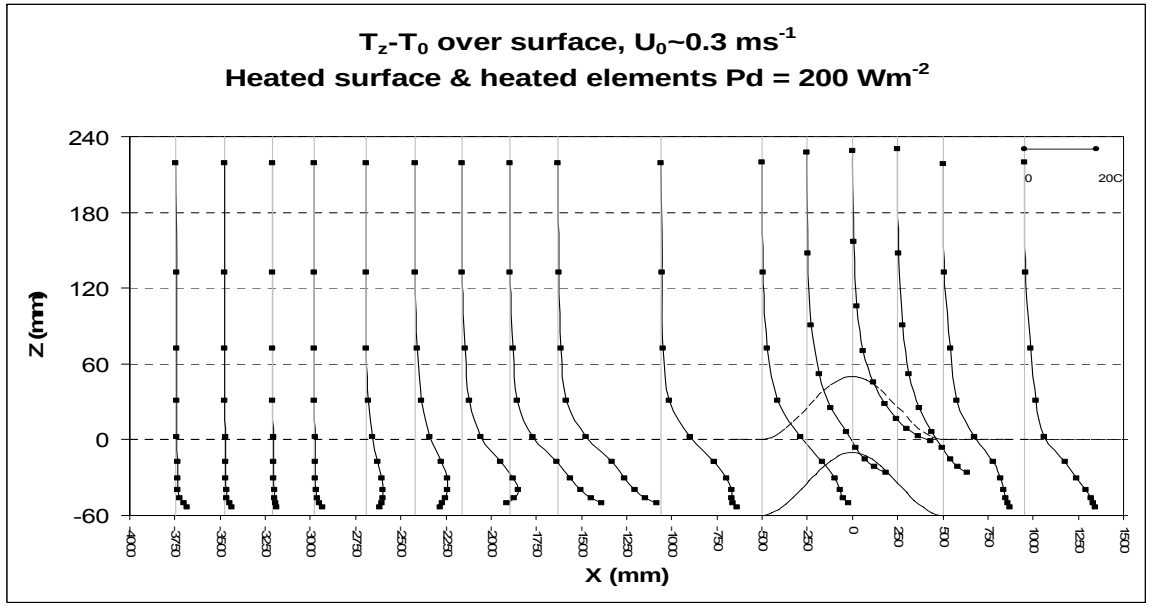

References

Harman, I. N., and J. J. Finnigan, 2007: A simple unified theory for flow in the canopy and roughness sublayer. *Bound. Layer Meteor.*, **123**, 339-363.

Kastner-Klein, P., M. W. Rotach, and E. Fedorovich, 2000: Experimental study of mean flow and turbulence characteristics in an urban roughness sublayer. *Proc. 14th AMS Symp. on Boundary Layer and Turbulence*. 7-11 August 2000, Aspen, Colorado, USA, 306-309.

Kastner-Klein, P., and M. W. Rotach, 2004: Mean flow and turbulence characteristics in an urban roughness sublayer. *Bound. Layer Meteor.*, **111**, 55-84.

Ohya, Y., and T. Uchida, 2003: Turbulence structure of stable boundary layers with a near-linear temperature profile. *Bound. Layer Meteor.*, **108**, 19-38.

Mestayer, P. G. and S. Anquetin, 1995: Climatology of cities. In: *Diffusion and Transport of Pollutants in Atmospheric Mesoscale Flows*, A. Gyr and F.-S. Rys (Eds.), Kluwer.

Thanks go to Yuji Ohya, Fernando Porté-Agel, Petra Klein, and John Finnigan

Laboratory studies deserve higher priority in our research agenda. Simply making this point is a big challenge, however, in a time when we are so overwhelmingly occupied with numerical modeling and simulation

John Wyngaard